Solvent-Mediated Redox Transformations of Ytterbium Bis(indenyl)-diazabutadiene Complexes

Alexander A. Trifonov,*[a] Elena A. Fedorova,[a] Vladimir N. Ikorskii,[b] Sebastian Dechert,[c][‡] Herbert Schumann,[c] and Mikhail N. Bochkarev[a]

Keywords: Diazadiene ligands / N ligands / Radical ions / Ytterbium

The reactions of diamagnetic $[(C_9H_7)_2Yb(THF)_2]$ (**2**) and [*rac*-$(CH_2\text{-}1\text{-}C_9H_6)_2Yb(THF)_2$] (**3**) with *t*BuN=CH–CH=N*t*Bu (DAD) in toluene result in the formation of the paramagnetic complexes $[(C_9H_7)_2Yb(DAD)]$ (**4**) and [*rac*-$(CH_2\text{-}1\text{-}C_9H_6)_2Yb$(DAD)] (**5**), respectively. The IR, UV/Vis, and ^{1}H NMR spectroscopic data, the magnetic properties, and the single-crystal X-ray diffraction studies of **4** and **5** indicate that in the solid state and in noncoordinating media both complexes are ytterbium(III) derivatives containing the DAD radical-anion, whereas the ^{1}H NMR and UV/Vis spectra of solutions of **4** and **5** in the coordinating solvent THF give evidence for divalent ytterbium. Recrystallization of **4** and **5** from THF/hexane results in the recovery of the starting ytterbium complexes **2** and **3** due to an unusual redox substitution of the radical anion of diazabutadiene by THF in the coordination sphere of ytterbium.

Introduction

During the past two decades, 1,4-disubstituted diazadienes have attracted considerable attention as useful ligands in transition metal chemistry due to their redox and coordination properties. The lone electron pair at both nitrogen atoms and the π-electrons of the C=N bonds allow theese molecules to act both as an n- and a π-electron donor. They can also coordinate metal atoms both as a neutral ligand[1] and, based on their quite pronounced electron affinity,[2] as a radical anion[3] or dianion[4] by accepting one or two electrons from the metal. Especially the ligand substituted at the nitrogen atoms with the bulky *tert*-butyl group (DAD) has been widely employed for the synthesis of stable complexes of electropositive lanthanides.[5] Considering the reduction state and the coordination mode of the DAD ligand, these compounds can be divided into two main groups. The first group contains homo- and hetero-ligated compounds containing the DAD radical anion coordinated to the lanthanide atom through two nitrogen atoms,[5] while in the second group the doubly reduced enediamido fragment is 2σ:π-bonded to the central metal atom.[6] Due to the low energy of the π*-orbital of diazadiene ligands,[2c] their complexes with ytterbium, a metal which has two stable oxidation states with a low Yb^{II}/Yb^{III} transformation potential,[7] are of particular interest with respect to intramolecular metal–ligand electron transfers. In our previous studies we have synthesized and structurally characterized the homoleptic ytterbium(III) complex $[(DAD)_3Yb]$ (**1**).[5c] In order to explain the results obtained for **1** from variable temperature magnetic measurements, a temperature-induced valence tautomerism has been suggested. Thus, complex **1** is assumed to exist as the divalent ytterbium derivative $[Yb^{II}(DAD^{-\cdot})_2(DAD^0)]$ at temperatures of 5 to 15 K, while in the temperature range 80 to 300 K the complex is transformed into the trivalent ytterbium compound $[Yb^{III}(DAD^{-\cdot})_3]$. Continuing our studies on intramolecular redox processes in DAD ytterbium complexes, we report here on unusual solvent-mediated redox transformations of the bis(indenyl)diazabutadieneytterbium complexes $[(Ind)_2Yb(DAD)]$.

[a] G. A. Razuvaev Institute of Organometallic Chemistry of Russian Academy of Sciences,
Tropinina 49, 603950 Nizhny Novgorod GSP-445, Russia
Fax: +7-8312-127-497
E-mail: trif@imoc.sinn.ru
[b] International Tomography Center of SB RAS,
Institutskaya str. 3a, 630090 Novosibirsk, Russia
E-mail: ikon@tomo.nsc.ru
[c] Institut für Chemie der Technischen Universität Berlin,
Straße des 17. Juni 135, 10623 Berlin, Germany
Fax: +49-30-3142-2168
E-mail: schumann@chem.tu-berlin.de
[‡] Present address: Institut für Anorganische Chemie, Georg August Universität Göttingen,
Tammannstr. 4, 37077 Göttingen, Germany
E-mail: dechert@chemie.uni-goettingen.de

Results and Discussion

The addition of *N*,*N*′-di-*tert*-butyl-1,4-diazabutadiene (DAD) in THF to THF solutions of $[(\eta^5\text{-Ind})_2Yb(THF)_2]$ [Ind = C_9H_7 (**2**), *rac*-$(CH_2\text{-}1\text{-}C_9H_6)$ (**3**)][8] does not cause any change in the color of the reaction mixtures and the ^{1}H NMR spectra of these mixtures show superposition of the spectra of the Yb^{II} complexes and of free DAD. Evapora-

  DOI: 10.1002/ejic.200401014

tion of the solvent in vacuo leaves a deep-red solid which, on addition of toluene, dissolves with formation of a brown (for **2**) or greenish-black solution (for **3**). The ^{1}H NMR spectra of these solutions show a set of broadened signals indicative of the presence of paramagnetic Yb^{III} species and radical anionic [DAD]$^{-\cdot}$ (Scheme 1).

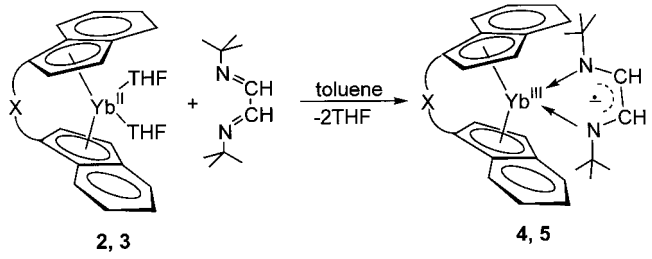

2, 3 **4, 5**

2, 4 X = no bridge; two seperated C_9H_7 ligands
3, 5 X = CH_2-CH_2

Scheme 1.

Cooling of the concentrated toluene solutions causes precipitation of the complexes [(η^5-Ind)$_2$Yb^{III}(DAD$^{-\cdot}$)] [Ind = C_9H_7 (**4**), *rac*-(CH_2-1-C_9H_6) (**5**)], which were isolated as dark-brown (**4**) and greenish-black (**5**) crystalline solids in yields of 74 and 81%, respectively. Both complexes are highly air- and moisture-sensitive, moderately soluble in toluene, and less soluble in hexane.

Crystals suitable for single-crystal X-ray diffraction studies were obtained by slow cooling of toluene solutions of **4** and **5** to –20 °C. Complex **5** crystallizes as a toluene solvate [*rac*-(CH_2-1-C_9H_6)$_2$Yb(DAD)](C_7H_8)$_{0.5}$. The molecular structures of **4** and **5** are depicted in Figures 1 and 2, respectively; crystal and structural refinement data are listed in Table 1.

In both compounds, the ytterbium atom is η^5-coordinated by the two cyclopentadienyl units of the indenyl ligands and the two nitrogen atoms of the radical anionic DAD ligand and adopts the geometry of a distorted tetrahedron. Complex **5** exists in the crystalline state only in the racemic form. The Yb–Cp$_{Centr.}$ distances in **4** [2.376(3) and 2.383(3) Å] as well as in **5** [2.371(2) and 2.383(2) Å] are shorter than those in the starting Yb^{II} complexes **2** [2.457(1) Å][9a,9b] and **3** [2.43(3)–2.45(3) Å][8b] and are close to the values reported for the indenylytterbium(III) derivatives [(1-C_4H_7-4,7-$Me_2C_9H_4$)$_2$Yb(μ-Cl)$_2$Li(THF)$_2$] [2.333(3) and 2.336(4) Å][10a] and [*meso*-(CH_2-1-C_9H_6)$_2$YbN($SiMe_3$)$_2$] [2.328(3) and 2.332(3) Å].[10b] The shortening of the Yb–Cp$_{Centr.}$ distances in **4** and **5** compared to those in **2** and **3** indicates the oxidation of the ytterbium atom from Yb^{II} to Yb^{III}.[11] However, in both cases the magnitude of the shortening is considerably less than would be expected on the basis of the difference in the ionic radii of Yb^{II} and Yb^{III} (0.155 Å). Further, it should be noted that the values of the Yb–Cp$_{Centr.}$ bond lengths in **4** and **5** lie between the corresponding values of [Cp$_2$Yb(DAD)] [2.324(7) and 2.334(4) Å][5g] and [Cp*$_2$Yb(DAD)] [2.401(2) and 2.414(2) Å][5h] and reflect the comparable steric demand of the cyclopentadienyl, pentamethylcyclopentadienyl, and indenyl ligands. Whereas the two Yb–N bond lengths in **4** [2.318(5) and 2.335(5) Å] as well as in **5** [2.321(4) and 2.343(5) Å] differ significantly between each other, the values still lie between the corresponding, almost equal values of [Cp$_2$Yb(DAD)] [2.309(9) and 2.306(9) Å][5g] and [Cp*$_2$Yb(DAD)] [2.385(4) and 2.394(3) Å].[5h] The Yb–N bond lengths in **4** and **5** are comparable to the lengths of the Yb^{III}–N coordination bonds in the compounds [Cp*$_2$Yb(bipy)] (2.32 Å),[12d] [{Cp*$_2$Yb(bipy)}$^+$-{Cp*$_2$YbCl$_2$}$^-$] (2.37 Å),[12d] [{Cp*$_2$Yb(phen)}$^+$(I)$^-$-(CH_2Cl_2)] (2.36 Å),[12d] and [Cp$_2$Yb($PzMe_2$)-($HpzMe_2$)] [2.360(6), 2.414(6) Å],[12e] but are much longer than the covalent Yb^{III}–N bonds in [(η^5-C_9H_7)$_2$YbN-($SiMe_3$)$_2$] [2.160(5), 2.163(5) Å],[12a] [(η^5-MeC_5H_4)$_2$Yb-(NPh_2)] [2.216(5) Å],[12b] [(η^5-MeC_5H_4)$_2$Yb(NPh_2)(THF)] [2.287(6) Å],[12b] and [{Li(THF)$_4$}{Yb(NPh_2)$_4$}] [2.188(9)–2.2401(9) Å].[12c] The bond lengths within the DAD ligand of **4** and **5** should indicate its radical-anionic character since an electron transfer to the LUMO of the ligand is expected to cause delocalization of the charge over the whole conjugated NCCN fragment, which involves changes in the bond lengths. Compared to the N=C [1.267(2) Å][13] and C–C bond lengths [1.467(2) Å][13] in the free DAD molecule, the N=C bonds in the DAD ligands of **4** [1.323(8) and 1.309(8) Å] and **5** [1.324(7) and 1.331(6) Å] are substantially elongated, while the C–C bonds [**4**: 1.412(9), **5**: 1.429(7) Å] are shortened and close to the values of aromatic carbon–carbon bonds.[14] This bonding situation is similar to that described for [Cp*$_2$Sm(DAD)],[5d] [Cp$_2$Yb(DAD)],[5g] and [Cp*$_2$Yb(DAD)],[5h] and proves the radical-anionic character of the DAD ligand in **4** and **5**. In summary, the struc-

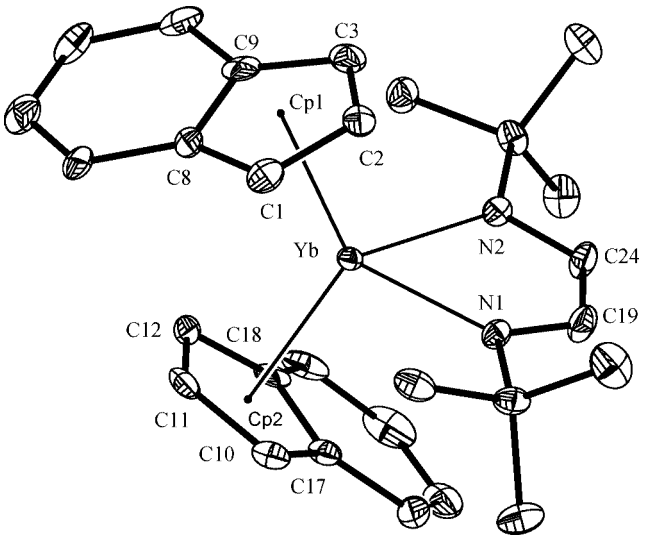

Figure 1. ORTEP diagram (30% probability thermal ellipsoids) of [(C_9H_7)$_2$Yb(DAD)] (**4**) showing the non-hydrogen-atom numbering scheme. Hydrogen atoms have been omitted for clarity. Relevant bond lengths [Å] and angles [°]: Yb–Cp1$_{Cent.}$ 2.383(3), Yb–Cp2$_{Cent.}$ 2.376(3), Yb–C1 2.630(7), Yb–C2 2.578(6), Yb–C3 2.616(6), Yb–C9 2.760(7), Yb–C8 2.770(6), Yb–C11 2.601(7), Yb–C12 2.605(6), Yb–C18 2.724(6), Yb–C17 2.741(6), Yb–C10 2.656(7), Yb–N2 2.318(5), Yb–N1 2.335(5), N1–C19 1.323(8), N2–C24 1.309(8), C19–C24 1.412(9); Cp1$_{Cent.}$–Yb–Cp2$_{Cent.}$ 125.44(11), N1–Yb–N2 74.35(19).

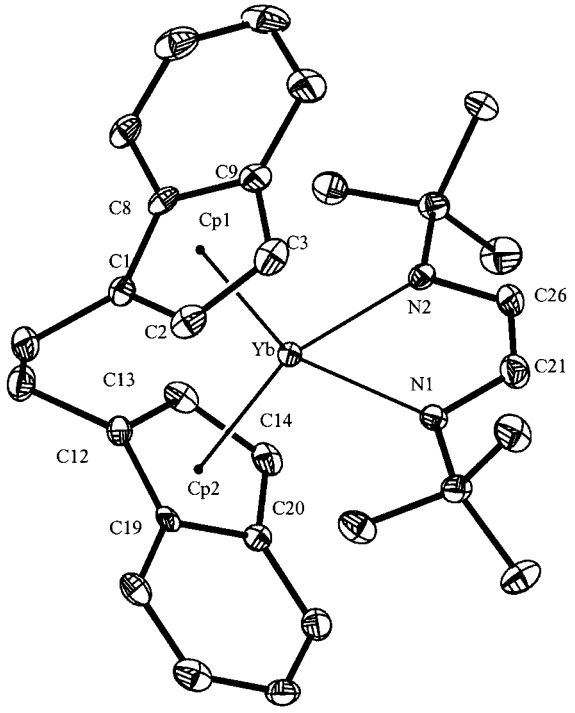

Figure 2. ORTEP diagram (30% probability thermal ellipsoids) of [*rac*-(CH_2-1-C_9H_6)$_2$Yb(DAD)] (**5**) showing the non-hydrogen-atom numbering scheme. Hydrogen atoms have been omitted for clarity. Relevant bond lengths [Å] and angles [°]: Yb–$Cp1_{Cent.}$ 2.371(2), Yb–$Cp2_{Cent.}$ 2.383(2), Yb–C1 2.646(5), Yb–C2 2.605(5), Yb–C3 2.623(5), Yb–C8 2.704(5), Yb–C9 2.719(5), Yb–C12 2.652(5), Yb–C13 2.590(5), Yb–C14 2.632(5), Yb–C19 2.750(5), Yb–C20 2.730(5), Yb–N1 2.321(4), Yb–N2 2.343(5), N1–C21 1.324(7), N2–C26 1.331(6), C21–C26 1.420(7); $Cp1_{Cent.}$–Yb–$Cp2_{Cent}$ 120.05(8), N1–Yb–N2 75.33(15).

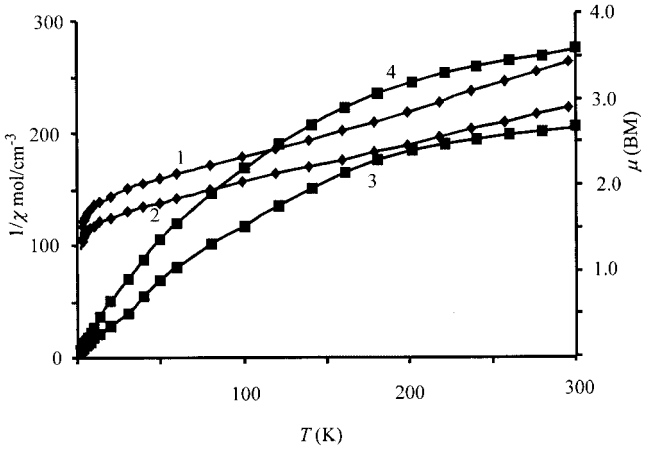

Figure 3. Thermal dependence of $1/\chi$ vs. T [K] and μ vs. T [K] for [(C_9H_7)Yb(DAD)] (**4**; curve 1: μ vs. T; curve 3: $1/\chi$ vs. T) and [*rac*-(CH_2-1-C_9H_6)$_2$Yb(DAD)] (**5**; curve 2: μ vs. T; curve 4: $1/\chi$ vs. T) at 5 kOe.

tural parameters of **4** and **5** are in agreement with the trivalent oxidation state of the ytterbium atom and the radical-anionic character of the DAD ligand. Unexpectedly, **4** and **5** are ESR silent in the temperature range 173 to 300 K in the solid state as well as in toluene solution. This fact is attributable either to a substantial broadening of the signal of the DAD radical anion in the field of the paramagnetic Yb^{III} ion or to antiferromagnetic coupling of the spin carriers.

Magnetic measurements of crystalline samples of **4** and **5** were carried out at 5 kOe in the temperature range 2 to 300 K. Plots of $1/\chi$ vs. T and μ vs. T are shown in Figure 3.

For **4** as well as for **5**, the measurements show a nonlinear dependence of the reciprocal value of the magnetic susceptibility χ as a function of temperature. The effective magnetic moments of the complexes increase from 1.6 μ_B (**4**) and 1.5 μ_B (**5**) at 2 K to 3.4 μ_B (**4**) and 3.0 μ_B (**5**) at 300 K. The values of the effective magnetic moments of **4** and **5** in benzene solution at 300 K, estimated according to the published procedure,[15] are in agreement with the data obtained for the crystalline samples by the SQUID method. The Yb^{III} ion has the electronic configuration $4f^{13}$ and is paramagnetic. The expected magnetic moment of Yb^{III} complexes is 3.8 μ_B at 5–30 K and 4.5 μ_B at 90–300 K;[16] the experimental values range from 3.4 to 4.9 μ_B.[17] An Yb^{III} complex that also contains a radical anion, as is suggested for **4** and **5**, should show a magnetic moment of 4.8 μ_B at room temperature provided that the spins of the two unpaired electrons do not interact. However, the experimental values of the magnetic moments obtained for **4** and **5** are considerably lower than the predicted ones, which could be caused either by redox tautomerism between paramagnetic [$(Ind)_2Yb^{III}(DAD^{\cdot-})$] and diamagnetic [$(Ind)_2Yb^{II}(DAD^0)$] molecules or antiferromagnetic coupling of the two unpaired electrons in [$(Ind)_2Yb^{III}(DAD^{\cdot-})$]. Recently, Andersen and co-workers studied the Yb^{III} complexes [Cp^*_2Yb(bipy)], [{1,3-t-$Bu_2C_5H_3$}$_2$Yb(phen)], and [Cp^*_2Yb(phen)] which contain an organic radical anion similar to **4** and **5**. They found effective magnetic moments at 300 K of 2.4, 3.4, and 4.0 μ_B, respectively. In order to interpret the low magnetic moments of these compounds, antiferromagnetic coupling between the spin carriers was postulated.[12d] Antiferromagnetic coupling between trivalent rare-earth ions and paramagnetic semiquinone ligands has been found also to be dominating for the series of complexes [Ln(DTBSQ)($HBPz_3$)$_2$] [Ln = Er, Tb, Dy, Yb; DTBSQ = 3,5-di-*tert*-butylsemiquinone, $HBPz_3$ = hydrotris(pyrazolyl)borate].[18] Hatfield and co-workers have described a strong exchange coupling between the lanthanide ions and the phthalocyaninato radical in bis(phthalocyaninato)lanthanide sandwich compounds [(Pc^{-2})Ln^{III}(Pc^{-1})] (Ln = Gd, Tb, Dy, Ho, Er, Tm, Yb, Lu). The value of the room-temperature magnetic moment for trivalent ytterbium antiferromagnetically coupled with an organic radical anion was calculated to be 3.46 μ_B.[19] Taking those results into account, the analysis of the $1/\chi$ vs. T and μ vs. T plots suggests that an antiferromagnetic spin interaction is a plausible reason for the low magnetic moments of **4** and **5**; however the available data do not allow us to exclude definitely the existence of redox tautomers.

The IR spectrum of neutral DAD shows two characteristic and strong absorption bands at 1620 and 1200 cm^{-1},

which are assigned to the ν(C=N) and ν(C–N) vibrations, respectively. In the IR spectra of **4** and **5** the absorption at 1200 cm^{-1} is still very strong, but the band at about 1600 cm^{-1} is very weak, which identifies the DAD ligand as a radical anion. The infrared data of **4** and **5** are consistent with those of [Cp$_2$Yb(DAD)][5g] and [Cp*$_2$Yb(DAD)],[5h] complexes which also contain the radical-anionic DAD ligand.

The UV/Vis spectra of **4** and **5** in hexane show strong absorptions at 318 and 335 nm, respectively, which correspond well with the strong band of (DAD$^{-\cdot}$)Na$^+$ at 325 nm, but differ from that of neutral DAD at 285 nm, thus giving further proof of the radical-anionic character of the DAD ligand (Figure 4). In contrast, the spectra of **4** and **5** recorded in the coordinating solvent THF at room temperature show evidence for the formation of free DAD and the respective THF-coordinated indenylytterbium(II) complexes [(C$_9$H$_7$)$_2$Yb(THF)$_2$] and [*rac*-(CH$_2$-1-C$_9$H$_6$)$_2$Yb(THF)$_2$].

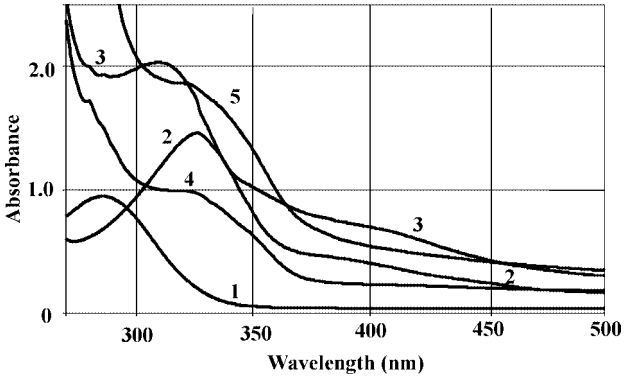

Figure 4. UV/Vis spectra. 1: DAD in hexane; 2: DAD$^{-\cdot}$Na$^+$ in THF; 3: [(C$_9$H$_7$)$_2$Yb(DAD)] (**4**) in hexane; 4: [(C$_9$H$_7$)$_2$Yb(DAD)] (**4**) in THF; 5: [(C$_9$H$_7$)$_2$Yb(THF)$_2$] (**2**) in THF.

According to the paramagnetism of **4** and **5**, their ^{1}H NMR spectra recorded in [D$_6$]benzene at 25 °C show a set of broadened signals that are substantially shifted with respect to those of comparable diamagnetic complexes (Figure 5 and Figure 6). The *tert*-butyl groups and the imino groups of the DAD ligand each gives rise to a singlet at δ = 27.90 (**4**) and 34.21 ppm (**5**) and a broad singlet at δ = –28.74 (**4**) and –18.53 ppm (**5**), respectively. The signals for the protons of the indenyl units appear at δ = 12.16, 10.41, –18.42, and –39.25 ppm in the intensity ratio of 2:2:2:1 for **4**, and at δ = 36.01, 32.74, 23.79, –0.85, –9.90, and –84.34 ppm with equal intensity for **5**. The proton signals of the ansa-ethylene group in **5** appear as two singlets at δ = –21.76 and –23.04 ppm. Variable temperature ^{1}H NMR measurements (–60 to 20 °C) of **4** in [D$_8$]toluene solution reveal a considerable temperature dependence of the chemical shift value of the imino protons (Figure 7), only a slight temperature dependence of the chemical shift value of the *tert*-butyl protons, and no temperature dependence of the chemical shift values of the indenyl protons.

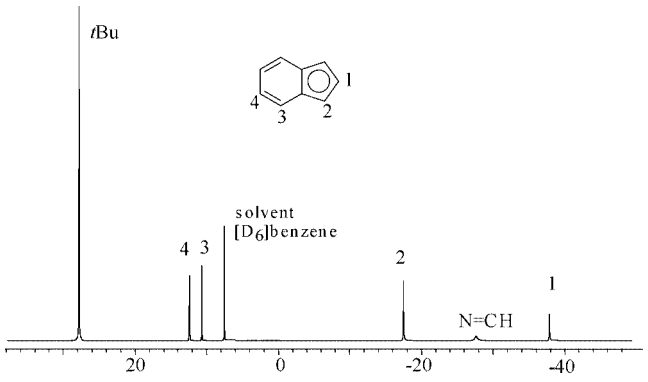

Figure 5. ^{1}H NMR spectrum of [(C$_9$H$_7$)$_2$Yb(DAD)] (**4**) in [D$_6$]benzene at 20 °C.

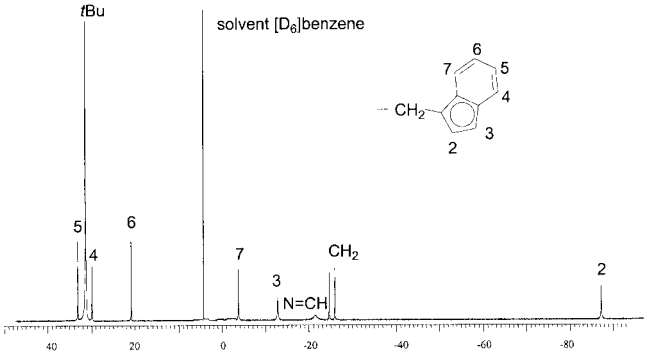

Figure 6. ^{1}H NMR spectrum of [*rac*-(CH$_2$-1-C$_9$H$_6$)$_2$Yb(DAD)] (**5**) in [D$_6$]benzene at 20 °C.

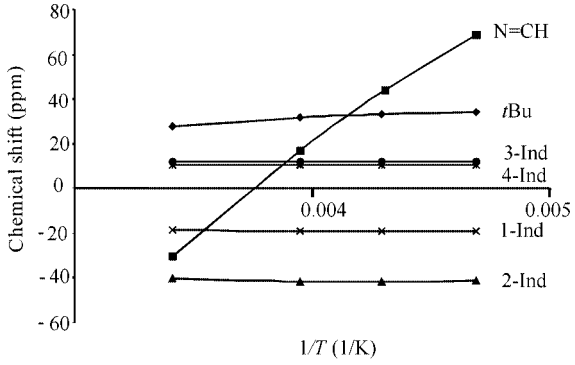

Figure 7. Variable temperature ^{1}H NMR spectroscopic data for [(C$_9$H$_7$)$_2$Yb(DAD)] (**4**) in [D$_8$]toluene: δ vs. 1/*T*.

The nature of the solvent influences the ^{1}H NMR spectra of **4** and **5** dramatically. Thus, in contrast to the ^{1}H NMR spectra of solutions of **4** and **5** in aromatic hydrocarbons, the spectra of solutions in the coordinating solvent [D$_8$]-THF show the sharp signals of DAD^0 and diamagnetic [(C$_9$H$_7$)$_2$Yb^{II}(THF)$_2$] or [*rac*-(CH$_2$-1-C$_9$H$_6$)$_2$Yb^{II}(THF)$_2$], respectively. It is worth noting that in the ^{1}H NMR spectra of solutions of **4** and **5** in [D$_8$]THF at 25 °C, recorded just after the preparation of the samples, the signals assigned to the diamagnetic Yb^{II} metallocenes (δ = 0 to 9 ppm) are still broad; they change to sharp signals with resolved coupling patterns only after about 6 h. The spectra of **4** and **5** in

CD_2Cl_2 cannot be recorded since the complexes react with this solvent.

In order to isolate the indenylytterbium(II) species that is present in the THF solutions, we added hexane at 20 °C to concentrated THF solutions of **4** and **5** and isolated the starting ytterbium(II) metallocenes $[(C_9H_7)_2Yb^{II}(THF)_2]$ (**2**) and [*rac*-$(CH_2$-1-$C_9H_6)_2Yb^{II}(THF)_2$] (**3**) in high yields (82 and 73%, respectively). *N*,*N*′-Di-*tert*-butyl-1,4-diazabutadiene was identified and isolated from the mother liquor by chromatographic methods in almost quantitative yields (Scheme 2).

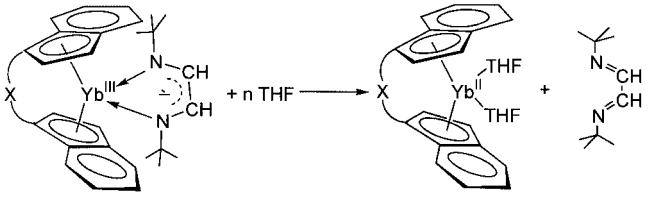

Scheme 2.

The above results allow the conclusion that complexes **4** and **5** exist as indenyl derivatives of trivalent ytterbium coordinated by the *N*,*N*′-di-*tert*-butyl-1,4-diazabutadiene radical anion $[(Ind)_2Yb^{III}(DAD^{-\cdot})]$ in the crystalline state as well as in noncoordinating solvents. Dissolution of **4** or **5** in coordinating solvents like THF causes displacement of the radical-anionic DAD ligand by THF molecules. This process implies an electron transfer from the diazadiene radical anion to the ytterbium(III) ion, resulting in the oxidation of the ligand to neutral DAD and reduction of Yb^{III} to Yb^{II}, followed by substitution of the neutral DAD ligand by two THF molecules. An analogous reductive substitution process has been established for the complex [Cp^*_2Yb-(DAD)], but not for [Cp_2Yb(DAD)] because of its shorter Yb–N distances.[5h] One can suppose that steric repulsion of the bulky indenyl and *N*,*N*′-di-*tert*-butyl-1,4-diazabutadiene ligands will be decisive for the examined reactions and the elongation and weakening of the Yb–N bonds in **4** and **5**. Hence, the energy of the Coulombic interaction between the $[(Ind)_2Yb^{III}]^+$ cationic species and the radical anion of diazadiene $DAD^{-\cdot}$ is comparable with that of the coordination bonds between Ind_2Yb^{II} and THF, and, as a result, the DAD ligand redox substitution becomes feasible. A similar behavior towards THF has been described by Evans and co-workers for decamethylsamarocene complexes with aromatic polycyclic ligands.[20] However, unlike the indenylytterbium complexes **4** and **5**, the samarium derivatives cannot be regenerated by removal of THF and addition of aromatic or aliphatic solvents.

Experimental Section

All experiments were performed in evacuated tubes, using standard Schlenk techniques, with rigorous exclusion of traces of moisture and air. THF, benzene, toluene, and hexane were purified by distillation from sodium/benzophenone ketyl and were condensed in vacuo prior to use. Indene (commercially available) was used after drying over molecular sieves. Commercially available 1,2-bis(indenyl)ethane was used as purchased (Dalchim). IR spectra were recorded as Nujol mulls on a Specord M80 spectrophotometer, and NMR spectra on a Bruker DPX200 spectrometer in [D_6]benzene, [D_8]THF, or [D_5]pyridine at 298 K. Chemical shifts for ^1H and ^{13}C NMR spectra were referenced internally using the residual solvent resonances and are reported relative to TMS. The UV/Vis spectra were recorded in evacuated quartz cuvettes on a Perkin–Elmer Lambda 25 spectrophotometer. The ESR spectra were measured on a Bruker ER 200D-1SRC instrument. GC analyses were performed with a Tzvet 530 gas chromatograph. Magnetic susceptibility measurements of solid samples were carried out on a SQUID magnetometer MPMS-5S from Quantum Design at 5 kOe. Magnetic measurements in benzene solution were performed according to the published procedure[15] on a Bruker DPX200 spectrometer. Lanthanide metal analyses were carried out by complexometric titration.

Synthesis of $[(C_9H_7)_2Yb(THF)_2]$ (2): A solution of indene (1.35 g, 11.68 mmol) in THF (10 mL) was added to a suspension of the naphthalene complex $[(C_{10}H_8)Yb(THF)_2]$ (2.60 g, 5.84 mmol) in THF (40 mL) and the reaction mixture was heated to 60 °C and stirred vigorously for 12 h. The resulting brown solution was filtered, THF was evaporated, and naphthalene was sublimed in vacuo at 60 °C. The solid residue was washed with hexane (2 × 20 mL) and recrystallized from THF/toluene (1:5 v/v). The precipitate was washed with cold toluene and dried in vacuo at room temperature to yield **2** as ruby-red crystals (2.36 g, 74%). $C_{26}H_{30}O_2Yb$ (547.5): calcd. C 57.03, H 5.52; found C 56.59, H 5.99. ^1H NMR (200 MHz, [D_5]pyridine): δ = 1.73 (m, 8 H, THF), 3.59 (m, 8 H, THF), 5.74 (d, $^3J_{H,H}$ = 3.2 Hz, 4 H, Ind), 6.2 (t, $^3J_{H,H}$ = 3.0 Hz, 2 H, Ind), 6.65 (m, 4 H, Ind), 7.31 (m, 4 H, Ind) ppm. $^{13}C\{^1H\}$ NMR (50 MHz, [D_5]pyridine): δ = 25.8 (THF), 67.9 (THF), 95.7 (Ind), 117.7 (Ind), 117.9 (Ind), 121.4 (Ind), 127.5(Ind) ppm. IR (KBr, Nujol): $\tilde{\nu}$ = 3060 cm^{-1} (w), 1320 (s), 1040(s), 860 (s), 760(s), 720 (s).

Synthesis of $[(CH_2$-1-$C_9H_6)_2Yb(THF)_2]$ (3): A solution of 1,2-bis-(indenyl)ethane (1.03 g, 4.02 mmol) in THF (10 mL) was added to a suspension of the naphthalene complex $[(C_{10}H_8)Yb(THF)_2]$ (1.79 g, 4.02 mmol) in THF (30 mL) and the reaction mixture was heated to 60 °C and stirred vigorously for 16 h. The resulting brown solution was filtered, THF was evaporated, and naphthalene was sublimed in vacuo at 60 °C. The solid residue was washed with hexane (2 × 20 mL) and recrystallized from THF/toluene (1:5 v/v). The precipitate was washed with cold toluene and dried in vacuo at room temperature to yield **3** as ruby-red crystals (1.89 g, 82%). $C_{28}H_{32}O_2Yb$ (573.6): calcd. C 58.63, H 5.62; found C 58.97, H 5.31. ^1H NMR (200 MHz, [D_5]pyridine): δ = 1.74 (br. s, 8 H, THF), 2.97 (s, 2 H, CH_2), 3.33 (s, 2 H, CH_2), 3.56 (br. s, 8 H, THF), 5.61 (d, $^3J_{H,H}$ = 4.0 Hz, 1 H, Ind), 5.75 (d, $^3J_{H,H}$ = 4.0 Hz, 1 H, Ind), 6.31 (m, 2 H, Ind), 6.48–6.69 (m, 4 H, Ind), 7.12 (m, 2 H, Ind), 7.55 (d, $^3J_{H,H}$ = 8.0 Hz, 1 H, Ind), 7.66 (d, $^3J_{H,H}$ = 8.0 Hz, 1 H, Ind) ppm. $^{13}C\{^1H\}$ NMR (50 MHz, [D_5]pyridine): δ = 25.8 (THF), 28.6 (CH_2), 28.7 (CH_2), 67.9 (THF), 94.5 (Ind), 94.8 (Ind), 112.4 (Ind), 115.1 (Ind), 117.1 (Ind), 117.3 (Ind), 119.1 (Ind), 119.8 (Ind), 121.0 (Ind), 121.2 (Ind), 123.9 (Ind), 125.3 (Ind), 125.6 (Ind), 127.2 (Ind), 127.8 (Ind) ppm. IR (KBr, Nujol): $\tilde{\nu}$ = 3060 cm^{-1} (w), 1320 (s), 1040(s), 860 (s), 760(s), 720 (s).

Synthesis of $[(C_9H_7)_2Yb(DAD)]$ (4): A solution of DAD (0.15 g, 0.89 mmol) in THF (2 mL) was added to a solution of **2** (0.49 g, 0.89 mmol) in THF (10 mL). The reaction mixture was stirred for

Table 1. Crystallographic data and structure refinement details for **4** and **5**.

	4	**5**
Empirical formula	$C_{24}H_{34}N_2Yb$	$C_{30}H_{36}N_2Yb{\cdot}0.5(C_7H_8)$
Formula mass	571.61	643.72
Crystal system	orthorhombic	monoclinic
Space group	$P2_12_12_1$ (no. 19)	$P2_1/c$ (no. 14)
a [Å]	9.2626(1)	18.6543(4)
b [Å]	14.3870(2)	8.3894(2)
c [Å]	18.1551(3)	17.9212(3)
β [°]	90	92.898(1)
V [Å^3]	2419.37(6)	2801.05(10)
Z	4	4
Density (calcd.) [g cm^{-3}]	1.569	1.526
μ [mm^{-1}]	3.882	3.363
T_{max}/T_{min}	0.5738/0.3079	0.9504/0.7035
F(000)	1144	1300
Crystal size [mm^3]	0.40 × 0.24 × 0.22	0.46 × 0.10 × 0.02
θ range [°]	1.81–27.50	2.19–27.50
Index ranges	$-12 \le h \le 11$ $-18 \le k \le 18$ $-23 \le l \le 14$	$-24 \le h \le 20$ $-9 \le k \le 10$ $-23 \le l \le 23$
Reflections collected	18803	20977
Independent reflections	5556 [R_{int} = 0.0896]	6425 [R_{int} = 0.0886]
Data/restraints/parameters	5556/0/286	6425/15/333
Goodness-of-fit on F^2	0.970	1.008
R indices [$I > 2\sigma(I)$]	R_1 = 0.0399 wR_2 = 0.0662	R_1 = 0.0434 wR_2 = 0.0619
R indices (all data)	R_1 = 0.0570 wR_2 = 0.0704	R_1 = 0.0834 wR_2 = 0.0710
Abs. struct. parameter	–0.024(15)	–
Largest diff. peak/hole [e Å^{-3}]	0.977/–1.649	0.817/–0.979

0.5 h at 20 °C. After the removal of THF in vacuo, toluene (10 mL) was added and the solution was heated to 60 °C for 1.5 h. The toluene was then evaporated in vacuo. Recrystallization of the solid residue from toluene (–20 °C) gave **4** as dark-brown crystals (0.37 g, 74%). $C_{28}H_{34}N_2Yb$ (571.6): calcd. C 58.83, H 6.00, Yb 30.27; found C 58.30, H 6.27, Yb 30.30. ^{1}H NMR (200 MHz, [D$_6$]benzene, 20 °C): δ = 27.90 (s, 18 H, Me$_3$C), 12.16 (s, 4 H, 3-Ind), 10.41 (s, 4 H, 4-Ind), –18.42 (s, 4 H, 2-Ind), –28.74 (s, 2 H, N=CH), –39.25 (s, 2 H, 1-Ind) ppm. IR (Nujol, KBr): $\tilde{\nu}$ = 3050 cm^{-1} (w), 1580 (w), 1365 (s), 1245 (s), 1200 (s), 770 (s), 740 (s).

Synthesis of [*rac*-(CH$_2$-1-C$_9$H$_6$)$_2$Yb(DAD)](C$_6$H$_5$CH$_3$)$_{0.5}$ (5): Similar to the procedure described for **4**, compound **5** was obtained from DAD (0.25 g, 1.49 mmol) in THF (5 mL) and **3** (0.86 g, 1.49 mmol) in THF (10 mL). Recrystallization from toluene afforded **5** as greenish-black crystals (0.77 g, 81%). $C_{33.5}H_{40}N_2Yb$ (643.7): calcd. C 62.50, H 6.26, Yb 26.88; found C 62.88, H 6.62, Yb 26.34. ^{1}H NMR (200 MHz, [D$_6$]benzene, 20 °C): δ = 36.01 (s, 2 H, 5-Ind), 34.21 (s, 18 H, Me$_3$C), 32.79 (s, 2 H, 4-Ind), 23.79 (s, 2 H, 6-Ind), –0.86 (s, 2 H, 7-Ind), –9.90 (s, 2 H, 3-Ind), –18.53 (s, 2 H, N=CH), –21.76 (s, 2 H, CH$_2$), –23.04 (s, 2 H, CH$_2$), –84.34 (s, 2 H, 2-Ind) ppm. IR (Nujol, KBr): $\tilde{\nu}$ = 3050 cm^{-1} (w), 1585 (w), 1370 (s), 1255 (s), 1200 (s), 780 (s), 7450 (s).

X-ray Crystallographic Study: The crystal data and details of data collection are given in Table 1. X-ray data were collected at –100 °C on a Siemens SMART CCD diffractometer (graphite monochromated Mo-K_α radiation, λ = 0.71073 Å, ω-scan technique) fitted with an area-detector. The structures were solved by direct methods using SHELXS-97[21] and refined on F^2 using all reflections with SHELXL-97.[22] The toluene solvent molecule in **5** is disordered about a crystallographic center of inversion. The C–C distances between ring carbon atoms were restrained to be equal. The atoms of the disordered part in **5** were refined isotropically, all other non-hydrogen atoms were refined anisotropically. The hydrogen atoms were placed in calculated positions and assigned using an isotropic displacement parameter of 0.08 Å^2. SADABS[23] was used to perform area-detector scaling and absorption corrections. The geometrical aspects of the structure were analyzed using the PLATON program.[24]

CCDC-257892 (**4**) and -257893 (**5**) contain the supplementary crystallographic data for this paper. These data can be obtained free of charge from The Cambridge Crystallographic Data Centre via www.ccdc.cam.ac.uk/data_request/cif.

Acknowledgments

This work was supported by the Russian Foundation for Basic Research (grant no. 03-03-32112), a grant of the President of the Russian Federation supporting scientific schools (no. 58.2003.3), the Fonds der Chemischen Industrie, and the Deutsche Forschungsgemeinschaft (Graduiertenkolleg "Synthetische, mechanistische und reaktionstechnische Aspekte von Metallkatalysatoren"). We gratefully acknowledge Dr. Yu. A. Kurskii for recording the NMR spectra and Prof. V. K. Cherkasov for recording the ESR spectra.

[1] a) K. Vrieze, *J. Organomet. Chem.* **1986**, *300*, 307–326; b) H. Bock, H. tom Dieck, *Chem. Ber.* **1967**, *100*, 228–246; c) J. Scholz, B. Richter, R. Goddar, K. Krueger, *Chem. Ber.* **1993**, *126*, 57–61.

[2] a) H. tom Dieck, I. W. Renk, *Chem. Ber.* **1971**, *104*, 110–130; b) H. tom Dieck, K.-D. Franz, F. Hoffmann, *Chem. Ber.* **1975**, *108*, 163–173; c) J. Reinhold, R. Benedix, P. Birner, H. Hennig, *Inorg. Chim. Acta* **1979**, *33*, 209–213.

[3] a) M. G. Gardner, G. R. Hanson, F. C. Lee, C. L. Raston, *Inorg. Chem.* **1994**, *33*, 2456–2461; b) F. G. N. Cloke, C. I. Dalby, M. J. Henderson, P. B. Hitchcock, C. H. L. Kennard, R. N.

Lamb, C. L. Raston, *J. Chem. Soc., Chem. Commun.* **1990**, 1394–1396; c) K.-H. Thiele, V. Lorenz, G. Thiele, P. Zoennchen, J. Scholz, *Angew. Chem.* **1994**, *106*, 1461–1463; *Angew. Chem. Int. Ed. Engl.* **1994**, *33*, 1372–1373.

[4] a) H. tom Dieck, J. Rieger, G. Fendesack, *Inorg. Chim. Acta* **1990**, *177*, 191–197; b) W. A. Hermann, M. Denk, W. Scherer, F.-R. Klingan, *J. Organomet. Chem.* **1993**, *444*, C21–C24; c) B. Richter, J. Scholz, J. Sieler, K.-H. Thiele, *Angew. Chem.* **1995**, *107*, 2865–2867; *Angew. Chem. Int. Ed. Engl.* **1995**, *34*, 2867–2869; d) F. G. N. Cloke, G. R. Hanson, M. J. Henderson, P. B. Hitchcock, C. L. Raston, *J. Chem. Soc., Chem. Commun.* **1989**, 1002–1003; e) J. Scholz, M. Dlikan, D. Stroehl, A. Dietrich, H. Schumann, K.-H. Thiele, *Chem. Ber.* **1990**, *123*, 2279–2285; f) J. Scholz, A. Dietrich, H. Schumann, K.-H. Thiele, *Chem. Ber.* **1991**, *124*, 1035–1039.

[5] a) F. G. N. Cloke, H. C. de Lemos, A. A. Sameh, *J. Chem. Soc., Chem. Commun.* **1986**, 1344–1345; b) F. G. N. Cloke, *Chem. Soc. Rev.* **1993**, *22*, 17–21; c) M. N. Bochkarev, A. A. Trifonov, F. G. N. Cloke, C. I. Dalby, P. T. Matsunaga, R. A. Andersen, H. Schumann, J. Loebel, H. Hemling, *J. Organomet. Chem.* **1995**, *486*, 177–182; d) A. Recknagel, M. Noltemeyer, F. T. Edelmann, *J. Organomet. Chem.* **1991**, *410*, 53–61; e) A. Scholz, K.-H. Thiele, J. Scholz, R. Weimann, *J. Organomet. Chem.* **1995**, *501*, 195–200; f) P. Poremba, F. T. Edelmann, *J. Organomet. Chem.* **1997**, *549*, 101–104; g) A. A. Trifonov, E. N. Kirillov, M. N. Bochkarev, H. Schumann, S. Muehle, *Russ. Chem. Bull.* **1999**, *48*, 382–384; h) A. A. Trifonov, Yu. A. Kurskii, M. N. Bochkarev, S. Muehle, S. Dechert, H. Schumann, *Russ. Chem. Bull.* **2003**, *52*, 601–606.

[6] a) A. A. Trifonov, L. N. Zakharov, M. N. Bochkarev, Yu. T. Struchkov, *Izv. Akad. Nauk, Ser. Khim.* **1994**, 148–151; b) H. Goerls, B. Neumueller, A. Scholz, J. Scholz, *Angew. Chem.* **1995**, *107*, 372–375; *Angew. Chem. Int. Ed. Engl.* **1995**, *34*, 673–676; c) J. Scholz, H. Goerls, H. Schumann, R. Weimann, *Organometallics* **2001**, *20*, 4394–4402.

[7] a) R. G. Finke, S. R. Keenan, D. A. Shirardi, P. L. Watson, *Organometallics* **1986**, *5*, 598–601; b) L. R. Morss, *Chem. Rev.* **1976**, *76*, 827–841; c) A. M. Bond, G. B. Deacon, R. H. Newnham, *Organometallics* **1986**, *5*, 2312–2316.

[8] The synthesis and characterization of complexes **2**[8a] and **3**[8b] have been previously reported. We describe here a new convenient synthesis for **2** and **3** by reaction of naphthaleneytterbium, $[(C_{10}H_8)Yb(THF)_2]$, with indene or 1,2-bis(indenyl)ethane in THF. a) G. B. Deacon, R. H. Newnham, *Aust. J. Chem.* **1985**, *38*, 1757–1765; b) A. V. Khvostov, B. M. Bulychev, V. K. Belsky, A. I. Sizov, *J. Organomet. Chem.* **1999**, *584*, 164–170.

[9] a) J. Z. Jin, Z. S. Jin, W. Q. Chen, Y. Zhang, *Chinese J. Struct. Chem. (Jiegou Huaxue)* **1993**, *12*, 241–245; b) A. A. Trifonov, M. N. Bochkarev, S. Dechert, H. Schumann, unpublished results.

[10] a) H. Schumann, D. Karasiak, S. Muehle, *Z. Anorg. Allg. Chem.* **2000**, *626*, 1434–1443; b) A. T. Gilbert, B. L. Davis, T. J. Emge, R. D. Broene, *Organometallics* **1999**, *18*, 2125–2132.

[11] R. D. Schannon, *Acta Crystallogr., Sect. A* **1976**, *32*, 751–767.

[12] a) E. Sheng, S. Wang, G. Yang, S. Zhou, L. Cheng, K. Zhang, Z. Huang, *Organometallics* **2003**, *22*, 684–692; b) Y. Wang, Q. Shen, F. Xue, K. Tu, *J. Organomet. Chem.* **2000**, *598*, 359–364; c) W.-K. Wong, L. Zhang, F. Xue, T. C. W. Mak, *Polyhedron* **1997**, *16*, 345–347; d) M. Schulz, J. M. Boncella, D. J. Berg, T. D. Tilley, R. A. Andersen, *Organometallics* **2002**, *21*, 460–472; e) X. Zhou, Z. Huang, R. Cai, L.-B. Zhang, L.-X. Zhang, X. Huang, *Organometallics* **1999**, *18*, 4128–4133.

[13] C. J. M. Huige, A. L. Spek, J. L. de Boer, *Acta Crystallogr., Sect. C* **1985**, *41*, 113–116.

[14] F. A. Allen, O. Konnard, D. G. Watson, L. Brammer, G. Orpen, R. Taylor, *J. Chem. Soc., Perkin Trans.* **1987**, 1–19.

[15] a) D. F. Evans, *J. Chem. Soc.* **1959**, 2003–2005; b) D. F. Evans, G. V. Fazakerley, R. F. Phillips, *J. Chem. Soc. A* **1971**, 1931–1934.

[16] a) M. Gerloch, E. C. Constable, *Transition Metal Chemistry*, VCH, Weinheim, **1995**; b) E. A. Boudreaux, L. N. Mulay, *Theory and Applications of Molecular Paramagnetism*; Wiley Interscience, New York, **1976**.

[17] W. J. Evans, M. A. Hozbor, *J. Organomet. Chem.* **1987**, *326*, 299–306.

[18] A. Caneschi, A. Dei, D. Gatteschi, S. Poussereau, L. Sorace, *Dalton Trans.* **2004**, 1048–1055.

[19] K. L. Trojan, J. L. Kendall, K. D. Kepler, W. E. Hatfield, *Inorg. Chim. Acta* **1992**, *198–200*, 795–803.

[20] a) W. J. Evans, T. A. Ulibarri, J. W. Ziller, *J. Am. Chem. Soc.* **1990**, *112*, 219–223; b) W. J. Evans, S. L. Gonzales, J. W. Ziller, *J. Am. Chem. Soc.* **1994**, *116*, 2200–2608.

[21] G. M. Sheldrick, *SHELXS-97 Program for the Solution of Crystal Structures*, University of Göttingen, **1990**.

[22] G. M. Sheldrick, *SHELXL-97 Program for the Refinement of Crystal Structures*, University of Göttingen, **1997**.

[23] G. M. Sheldrick, *SADABS Program for Empirical Absorption Correction of Area Detector Data*, University of Göttingen, **1996**.

[24] A. L. Spek, *PLATON A Multipurpose Crystallographic Tool*, University of Utrecht, **2000**.

Received: December 10, 2004
Published Online: June 9, 2005

